High-aspect-ratio germanium zone plates fabricated by reactive ion etching in chlorine

Magnus Lindblom,[a] Julia Reinspach, Olov von Hofsten, Michael Bertilson, Hans M. Hertz, and Anders Holmberg
Department of Applied Physics, Royal Institute of Technology, Stockholm SE-106 91, Sweden

(Received 6 November 2008; accepted 2 February 2009; published 9 March 2009)

This article describes the fabrication of soft x-ray germanium zone plates with a process based on reactive ion etching (RIE) in Cl_2. A high degree of anisotropy is achieved by sidewall passivation through cyclic exposure to air. This enables structuring of higher aspect ratios than with earlier reported fabrication processes for germanium zone plates. The results include a zone plate with a 30 nm outermost zone width and a germanium thickness of 310 nm having a first-order diffraction efficiency of 70% of the theoretical value. 25 nm half-pitch gratings were also etched into 310 nm of germanium. Compared to the electroplating process for the commonly used nickel zone plates, the RIE process with Cl_2 for germanium is a major improvement in terms of process reproducibility. © *2009 American Vacuum Society.* [DOI: 10.1116/1.3089371]

I. INTRODUCTION

Zone plates are diffractive lenses widely used in the x-ray spectral range for high-resolution focusing and imaging.[1] For the soft x-ray range, electroplated nickel zone plates presently dominate due to their high diffraction efficiency. In the present article we report on a new fabrication process for germanium zone plates based on reactive ion etching (RIE) with Cl_2. The relative simplicity of this fabrication process makes germanium zone plates an attractive alternative to nickel zone plates.

In order to obtain a high diffraction efficiency, the optical material of a zone plate should be strongly phase shifting and weakly absorbing.[2] For soft x-rays, nickel and germanium have long been identified as suitable materials in this respect. In Fig. 1 their theoretical diffraction efficiencies at $\lambda = 2.88$ nm are graphed as a function of the material thickness. Nickel, which is a common material for soft x-ray zone plates, can provide a higher efficiency than germanium. Unfortunately, there is no applicable dry-etch process for nickel, and the fabrication therefore relies on electroplating into a structured mold. The electroplating is difficult to control in comparison to the other process steps and some of the problems concern control of the mass distribution[3–6] and the deposition rate,[7] pattern stability,[8–10] and adhesion of the plating mold. Germanium, on the other hand, can be structured to high aspect ratios by plasma etching. It used to be a common zone-plate material and there are several reports in literature from the period 1987–2000.[11–18] The fabrication during that time was based on RIE of germanium with $CBrF_3$, which is an ozone-depleting gas that has been taken off the market. Chlorine, however, is available and, in the present article, we show that the RIE of germanium with Cl_2 can be highly anisotropic and it is therefore well suited for zone-plate fabrication.

II. FABRICATION PROCESS

The fabrication is based on a trilayer process, as illustrated in Fig. 2. It comprises an electron-beam-lithography step for patterning and two steps of RIE for the subsequent pattern transfer into the germanium film. For the fabrication of the zone plates and the grating lines presented in this work, 50 nm thick silicon nitride membranes were used as substrates. These were coated with a 10 nm titanium etch stop. The trilayer itself consisted of 310 nm of germanium, a 10 nm titanium hard mask, and 50 nm of e-beam resist (ZEP7000, Nippon Zeon Co.). The e-beam resist was spun cast and then baked for 30 min at 170 °C. The titanium and the germanium layers were deposited by e-beam evaporation in an Auto 306 system (Edwards Ltd.) under high-vacuum conditions (base pressure of 2×10^{-6} mbar) and without temperature control of the substrate. The deposition rates were approximately 1 and 0.3–0.4 Å/s for titanium and germanium respectively.

The samples were patterned by e-beam lithography at 25 keV (Raith 150 system) and developed in hexyl acetate for 30 s. The pattern transfer to the titanium hard mask was done by RIE with BCl_3 (Oxford Plasmalab 80+) under the following conditions: 80 W sample rf power ($0.33\ W/cm^2$), 15 mTorr pressure, and 10 sccm BCl_3 flow. The etch time was 110 s. The final step, the pattern transfer into the germanium layer, was performed by RIE with Cl_2 (Oxford Plasmalab 100). A helium back side pressure of 5 Torr was applied and the working electrode was kept at 20 °C. The membranes were placed on a silicon carrier wafer but were not thermally connected to it. The etching was done using 25 W ($0.1\ W/cm^2$) of sample rf power, 2 mTorr pressure, and 10 sccm gas flow. The total etch time was 3 min but it was divided into four steps: 30, 30, 60, and 60 s. The sample was unloaded between each etch step for sidewall passivation.

Sidewall passivation was needed for linewidths in the range of 30 nm for which the aspect ratio was about 10:1. Since oxides normally etch slowly in Cl_2 plasmas, isotropic etching can be inhibited by oxidation of the germanium sur-

[a]Electronic mail: magnus.lindblom@biox.kth.se

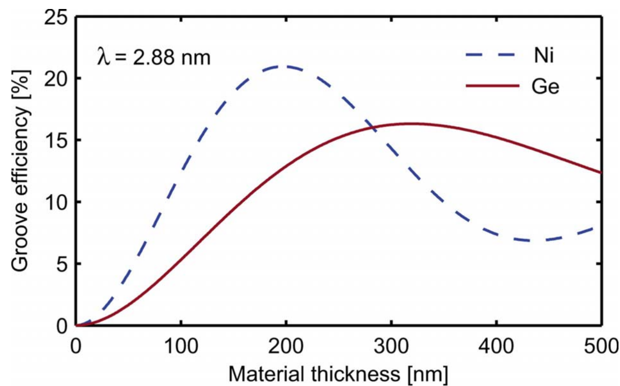

FIG. 1. (Color online) Theoretical first-order groove efficiency at $\lambda=2.88$ nm as a function of thickness for nickel and germanium gratings. Optically thin gratings are assumed.

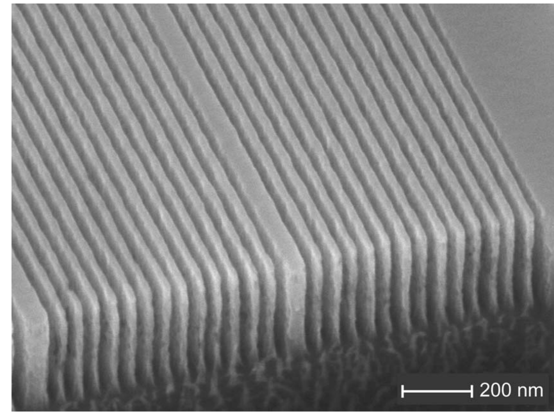

FIG. 3. SEM image of gratings with 25 nm half-pitch in 310 nm thick germanium (52° tilt angle). The aspect ratio of the lines is 12.4:1.

face. The oxide layer at the bottom of the trenches is then cleared by the ion bombardment so that the etching can proceed vertically, while the sidewalls remain protected. The most successful passivation method was to simply unload the sample and expose it to air between the etch steps. No lateral etch rate could be detected using this method and the degree of anisotropy was determined by the length of the etch interval. However, grass formation was observed for etch intervals shorter than 30 s and occasionally when only 30 s intervals were used. This problem was avoided by combining 30 and 60 s intervals as described above. In Fig. 3, which shows a grating etched for 30+30+60+60 s, it is possible to see the effect of the increased length of the later etch intervals. The upper part of the lines is thicker and the sidewalls are more vertical than for the lower part where the etch process has been more isotropic.

Other schemes to inhibit sidewall etching were also investigated. Oxidation with O_2 plasma and addition of 5% oxygen to the feed gas (1 sccm O_2 and 19 sccm Cl_2 flow rate) both prevented sidewall etching but they also resulted in excessive grass formation. A third method was attempted in which a flow of oxygen (50 sccm at a chamber pressure of 90 mTorr) was applied for up to 10 min between the Cl_2 etch intervals. This did not have a noticeable passivating effect.

III. RESULTS AND DISCUSSION

With the process described in the previous section, a zone plate with 30 nm outermost zone width and a germanium thickness of 310 nm was fabricated (cf. Fig. 4). The zone-plate diameter was 56 μm. The first-order diffraction efficiency was measured in a laboratory laser-plasma based arrangement operating at $\lambda=2.88$ nm.[19] At this wavelength, the average efficiency for the entire zone plate area, including substrate absorption, was 8.1%. Taking into account the transmission of the substrate, consisting of 50 nm of Si_3N_4 and 10 nm of Ti, an average groove efficiency of 11.5% was obtained. For a germanium thickness of 310 nm and $\lambda=2.88$ nm, this corresponds to approximately 70% of the theoretical efficiency as calculated with the formula given by Kirz.[20] The radial variation in the diffraction efficiency is displayed in Fig. 5. As expected, due to increasing fabrication difficulties, the efficiency decreases with the radially shrinking zone width. The abrupt decrease in efficiency over the last micrometer does not, however, reflect a reduction in the pattern quality. This is a blurring effect in the measurement,[19] which causes the data to extend further than the zone-plate radius. It should also be noted that the innermost part of the graph in Fig. 5 originally contained the

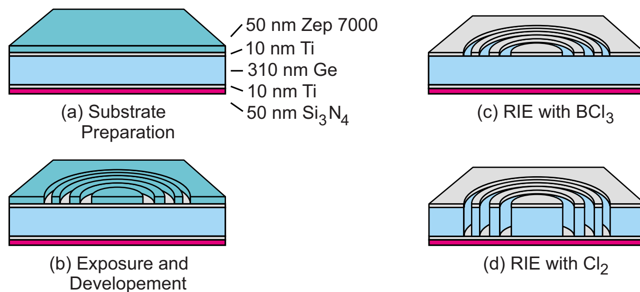

FIG. 2. (Color online) Steps of the fabrication process. First, the material stack is prepared by physical vapor deposition and spin coating (a). The zone-plate pattern is then written by e-beam lithography (b) and transferred to the titanium hard mask by RIE with BCl_3 (c). The final step is the RIE with Cl_2 into the germanium layer (d).

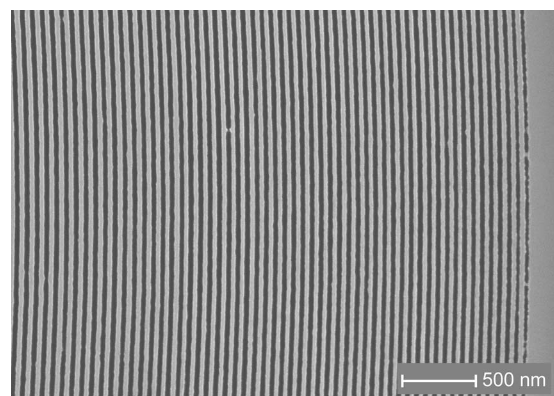

FIG. 4. SEM image showing the outer part of a zone plate with 30 nm outermost zone width fabricated in 310 nm of germanium.

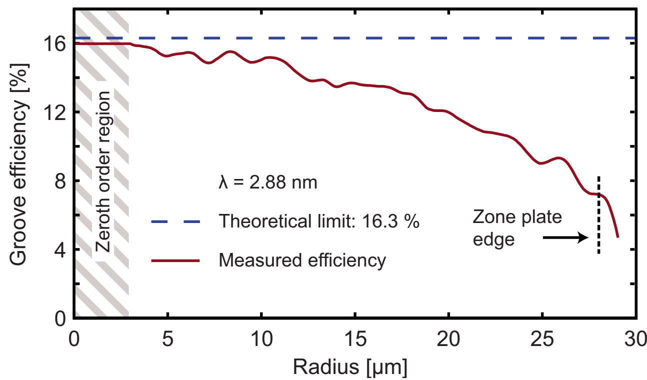

FIG. 5. (Color online) Radial dependence of the first-order groove efficiency measured at $\lambda = 2.88$ nm for a 310 nm thick germanium zone plate with 30 nm outermost zone width. The average groove efficiency was 11.5%, which corresponds to 70% of the theoretical value. The edge of the zone plate (radius of 28 μm) is marked in the figure. The data beyond the edge correspond to a blurring in the measurement.

zeroth-order from the zone plate. The data for a radius of less than 3 μm were therefore replaced by assuming a constant efficiency in this region. This is of little consequence for the measurement since this area only corresponds to 1% of the total area of the zone plate.

The process has a potential for finer linewidths and higher aspect ratios. This is demonstrated in Fig. 3, where a grating with 25 nm half-pitch in 310 nm of germanium is shown. The aspect ratio of the lines is 12.4:1, which is higher than what has been reported for the zone plate fabrication process based on RIE with $CBrF_3$.

Finally, a comment is made regarding the durability of the Ti hard mask in the Cl_2 plasma. Although the composition of the films was not measured, it was clear that it was not pure titanium since the films lacked the characteristic metallic appearance that Ti films deposited at ultrahigh-vacuum conditions have. In addition, the etch rate of the hard mask was low, ~1.6 nm/min, and independent of the etch time (up to 12 min). This could be explained if, for instance, the film was oxidized during deposition. Pure titanium is etched by Cl_2 plasmas, but titanium oxides on the other hand and, in particular, the native TiO_2, are very resistant.[21–23] The etch resistance of a hard mask of pure titanium would be reliant on the presence of native oxide (2–5 nm thick[24,25]) and the etch rate would therefore be expected to be time dependent. In that case, a cyclic oxidation is likely to be useful for reinforcement of the hard mask as well as for sidewall passivation of the germanium.

In summary, we have demonstrated a process based on RIE with Cl_2 for the fabrication of germanium zone plates. The anisotropy of the germanium etch is very high due to the application of sidewall passivation. The presented process therefore enables the fabrication of zone plates with high diffraction efficiency for soft x-rays without the need for electroplating as for the commonly used nickel zone plates.

ACKNOWLEDGMENTS

The authors gratefully acknowledge the financial support of the Swedish Science Research Council, the Swedish Foundation for Strategic Research, the Wallenberg Foundation, and the Göran Gustafsson Foundation.

[1] *X-Ray Microscopy*, edited by S. Aoki, Y. Kagoshima, and Y. Suzuki (The Institute of Pure and Applied Physics, Tokyo, Japan, 2006), Vol. 7.
[2] A. G. Michette, *Optical Systems for Soft X-Rays* (Plenum, New York, 1986).
[3] S. Mehdizadeh, J. Dukovic, P. C. Andricacos, L. T. Romankiw, and H. Y. Cheh, J. Electrochem. Soc. **140**, 3497 (1993).
[4] M. Peuker, Appl. Phys. Lett. **78**, 2208 (2001).
[5] M. Lindblom, H. M. Hertz, and A. Holmberg, J. Vac. Sci. Technol. B **24**, 2848 (2006).
[6] A. C. West, M. Matlosz, and D. Landolt, J. Electrochem. Soc. **138**, 728 (1991).
[7] A. Holmberg, M. Lindblom, and H. M. Hertz, J. Vac. Sci. Technol. B **24**, 2592 (2006).
[8] D. Weiss, M. Peuker, and G. Schneider, Appl. Phys. Lett. **72**, 1805 (1998).
[9] D. L. Olynick, B. D. Harteneck, E. Veklerov, M. Tendulkar, J. A. Liddle, A. L. D. Kilcoyne, and T. Tyliszczak, J. Vac. Sci. Technol. B **22**, 3186 (2004).
[10] M. Lindblom, H. M. Hertz, and A. Holmberg, Microelectron. Eng. **84**, 1136 (2007).
[11] R. Hilkenbach, J. Thieme, P. Guttmann, and B. Niemann, *X-Ray Microscopy II* (Springer, Heidelberg, Germany, 1988), p. 95.
[12] C. David, J. Thieme, P. Guttmann, G. Schneider, D. Rudolph, and G. Schmahl, Optik (Stuttgart) **91**, 95 (1992).
[13] J. Thieme, D. Rudolph, G. Schmahl, P. Guttmann, B. Greinke, and M. Diehl, *X-Ray Microscopy III* (Springer, Heidelberg, Germany, 1992), p. 83.
[14] C. David, N. Fay, R. Medenwaldt, M. Diehl, and J. Thieme, *Proceedings of the Fourth International Conference on X-Ray Microscopy* (Institute of Microelectronics Technology, Chernogolovka, Russia, 1994), p. 536.
[15] G. Schneider, T. Schliebe, and H. Aschoff, J. Vac. Sci. Technol. B **13**, 2809 (1995).
[16] C. David, B. Kaulich, R. Medenwaldt, M. Hettwer, N. Fay, M. Diehl, and J. Thieme, J. Vac. Sci. Technol. B **13**, 2762 (1995).
[17] S. J. Spector, C. J. Jacobsen, and D. M. Tennant, J. Vac. Sci. Technol. B **15**, 2872 (1997).
[18] T. Schliebe and G. Schneider, *X-Ray Microscopy and Spectromicroscopy* (Springer, Heidelberg, Germany, 1998), p. IV-3.
[19] M. Bertilson, P. A. C. Takman, U. Vogt, A. Holmberg, and H. M. Hertz, Rev. Sci. Instrum. **78**, 026103 (2007).
[20] J. Kirz, J. Opt. Soc. Am. **64**, 301 (1974).
[21] A. M. Muthukrishnan, K. Amberiadis, and A. ElshabiniRiad, J. Electrochem. Soc. **144**, 1780 (1997).
[22] F. Fracassi and R. Dagostino, Pure Appl. Chem. **64**, 703 (1992).
[23] R. d'Agostino, F. Fracassi, C. Pacifico, and P. Capezzuto, J. Appl. Phys. **71**, 462 (1992).
[24] S. L. Lehoczky, R. J. Lederich, and J. J. Bellina, Thin Solid Films **55**, 125 (1978).
[25] C. Sittig, M. Textor, N. D. Spencer, M. Wieland, and P. H. Vallotton, J. Mater. Sci.: Mater. Med. **10**, 35 (1999).